PCCP

Eigenvalue spectrum of the master equation for hierarchical dynamics of complex systems

Yaakov Levy,[a] Joshua Jortner[a] and R. Stephen Berry[b]

[a] *Department of Chemical Physics, School of Chemistry, Tel Aviv University, Ramat Aviv, Tel-Aviv 69978, Israel*
[b] *Department of Chemistry and The James Franck Institute, The University of Chicago, Chicago, Illinois 60637*

Received 10th April 2002, Accepted 7th August 2002
First published as an Advance Article on the web 11th September 2002

We explored the eigenvalue spectra of the kinetic matrix which defines the master equation for the complex kinetics of the analogous polypeptides (linear Ala6, cyclic Ala6, and charged Ala6). For each system we obtained the entire eigenvalue spectrum as well as the histograms of the weighted eigenvalue spectra, where each relaxation mode is weighted by the overlap between the initial probability vector and the corresponding eigenvector. It was found that the spectra of the weighted eigenvalues were significantly filtered in comparison to those of the unweighted eigenvalues, indicating that the decay is described by a small number of eigenvalues. The important eigenvalues which are extracted from the weighted eigenvalues spectra are in good agreement with the characteristic lifetimes for the kinetics of each system, as found by the fitting of the energy relaxation temporal profiles to multiexponential functions. Moreover, a partial correlation is found between the relative heights of the contributions of the important eigenvalues and the preexponential factors obtained by the fitting. In addition, we applied the spectra of the weighted eigenvalues to study the effect of the initial population distribution on the dynamics and also to infer which minima provide the dominant contributions to a specific relaxation mode. From the latter results one can infer whether the multiexponential relaxations represent sequential or parallel processes. This analysis establishes the interrelationship between the topography and topology of the energy landscapes and the hierarchy of the relaxation channels.

1. Introduction

The kinetics of complex systems such as clusters, peptides and proteins, ranges from a simple exponential relaxation to stretched exponential or asymptotic power-law relaxations.[1–5] In other cases, a multiple exponential kinetics better describes the kinetics of such systems.[6,7] The distinct dynamics originates from the differences in topographies and topologies of the energy landscapes of the systems.[8–19] Various energetic and entropic barriers, the different numbers and sizes of basins, the existence of kinetic traps, and different degrees of landscape ruggedness may dictate distinct dynamics.[20–25]

The dynamics and kinetics of clusters[12,13,26,27] and small polypeptides[13–17,28,29] were studied with the aid of the master equations, based on a detailed characterization of their energy landscapes. The power of the master equation approach is that it can be used to study the kinetics on a timescale considerably longer than that accessible through direct molecular dynamics simulations. In addition, the master equation describes the relaxation of an ensemble over a range of temperatures without the need for explicit averaging over the separate trajectories. The prerequisite for any master equation study is a knowledge of the underlying energy landscape and of the transition rates between the minima. Recently, the master equation was applied to the dynamics of three analogous hexapeptides, linear hexaalanine (Ala6), cyclic hexaalanine (cyc-Ala6), and charged hexaalanine (chrg-Ala6), which differ due to different topographical and topological properties of their energy landscapes.[15,16] The kinetics of the three molecular systems were shown to be nonexponential in the temperature range 400–600 K. The kinetics of each system was well characterized by multiple exponential functions with fast and slow events. The kinetics for the three systems differs with respect to the timescales and to the degrees of their hierarchy.

The purpose of this study is to present an alternative way to interpret the solutions of the master equation and extract information from them about the dynamics of complex systems. The ordinary use of the master equation follows the time evolution of a specific property (*e.g.*, the potential energy) towards its equilibrium value. From the relaxation profiles the timescales and the kinetic mechanisms can be studied. We advance a simpler inspection method of the kinetic properties by analyzing the eigenvalue spectra and the eigenvectors of the kinetic matrix, which define the master equation. While total eigenvalue spectra of the master equation were already presented for alkali halides and for rare gas clusters,[26,27] the present study of the weighted eigenvalue spectra provides a wealth of dynamic information. We propose and demonstrate that some central characteristics of the dynamics and the kinetics of a complex system can be extracted from the weighted eigenvalue spectra and from the eigenvectors of the kinetics matrix prior to the time integration of the master equation, without the need of fitting the relaxation profile to various functions.

2. The master equation

The master equation represents a fundamental statistical mechanical approach to kinetic transitions among a multitude of states. It is a loss–gain equation that describes the time evolution of the probability $P_i(t)$ for finding the system

 DOI: 10.1039/b203534k

in a state i.[30,31] In the description of the energy landscape, local minima represent conformational states of the cluster or peptide molecule, i, while the saddle points (which represent transition states) determine the state-to-state transition rates. The basic form of the master equation, which provides a connection between the topography of the energy landscape and the system's kinetic behavior, is

$$\frac{\mathrm{d}P_i(t)}{\mathrm{d}t} = \sum_j [W_{ij}P_j(t) - W_{ji}P_i(t)] \tag{1}$$

where W_{ij} is the transition probability from state j to state i. This equation can be rewritten in matrix form $\dot{\boldsymbol{P}}(t) = \tilde{\boldsymbol{W}}\boldsymbol{P}(t)$, where $\boldsymbol{P}(t)$ is the probability vector at time t, and its formal solution is $\boldsymbol{P}(t) = \exp(t\tilde{\boldsymbol{W}})\boldsymbol{P}(0)$. In this formulation the transition matrix elements are defined as

$$\tilde{\boldsymbol{W}}_{ij} = W_{ij} - \delta_{ij}\left(\sum_k W_{ki}\right) \tag{2}$$

The properties of the $\tilde{\boldsymbol{W}}$ matrix are $\tilde{W}_{ij} \geqslant 0$ for $i \neq j$ and the sum over each column is zero; namely, $\sum_i \tilde{W}_{ij} = 0$ for all j. Given the knowledge of the minima and the transition states on the energy landscape it is possible to use the transition state theory (TST) (among other methods) to evaluate the transition matrix elements (rate constants k_{ij}), *i.e.*,

$$k_{ij} \equiv \tilde{\boldsymbol{W}}_{ij} = \frac{kT}{h}\frac{Q_{ij}^{\ddagger}}{Q_j}\exp\left(-E_{ij}^{\ddagger}/kT\right) \tag{3}$$

where k is the Boltzmann constant, h the Planck constant, Q_j the partition function of the 'reactant' state, $Q_{ij}^{\ddagger}$ the partition function of the transition state and $E_{ij}^{\ddagger}$ is the barrier height measured relative to state j.

To follow the time evolution of the population probability at each minimum, $P_i(t)$, it is necessary to solve the master equation, eqn. (1). This can be done by expanding the probability vector $\boldsymbol{P}(t)$ in terms of the eigenvectors ($\boldsymbol{S}_i$), and the eigenvalues (λ_i) of the transition matrix $\tilde{\boldsymbol{W}}$. The time evolution of the probability vector $\boldsymbol{P}(t)$ can be written as

$$P_i(t) = \sqrt{P_i^{\mathrm{eq}}}\sum_{k=1}^{n} C^k S_i^k \mathrm{e}^{\lambda_k t} \tag{4}$$

where

$$C^k = \sum_{j=1}^{n} S_j^k \frac{P_j(0)}{\sqrt{P_j^{\mathrm{eq}}}} \tag{5}$$

All $\lambda_k < 0$ for $2 \leqslant k \leqslant n$ and $\lambda = 0$ for $k = 1$. As $t \to \infty$, only the $k = 1$ term in eqn. (4) survives, and $\boldsymbol{P}(t) \to \boldsymbol{P}^{\mathrm{eq}}$, where $\boldsymbol{P}^{\mathrm{eq}}$ is the probability vector at equilibrium. This limit defines the baseline to which the remaining modes decay exponentially. Thus, eqn. (4) can be rewritten as

$$P_i(t) = P_i^{\mathrm{eq}} + \sqrt{P_i^{\mathrm{eq}}}\sum_{k=2}^{n} C^k S_i^k \mathrm{e}^{\lambda_k t} \tag{6}$$

The term $\sqrt{P_i^{\mathrm{eq}}}C^k S_i^k$ is the contribution of mode k, with eigenvalue λ_k, to the evolution of the probability minimum i. The size of this contribution depends on component i of eigenvector k, S_i^k, and on the coefficient C^k, which is a weighted overlap between the initial probability vector, $\boldsymbol{P}(0)$, and eigenvector k, $\boldsymbol{S}^k$ (eqn. (5)). The sign of the product of these two quantities determines whether the mode makes an increasing or a decreasing contribution with time.

The evolution of the probability vector towards $\boldsymbol{P}^{\mathrm{eq}}$ is expressed macroscopically by the relaxation of an overall property A to its equilibrium value A^{eq}. If this property has a well defined value in the master equation for each state i, the expectation value is a weighted average which can be expressed as a function of time using eqn. (4):

$$\langle A(t)\rangle = \sum_{i=1}^{n} A_i P_i(t) = \sum_{i=1}^{n} A_i\sqrt{P_i^{\mathrm{eq}}}\sum_{k=1}^{n} C^k S_i^k \mathrm{e}^{\lambda_k t} \tag{7}$$

3. Results and discussion

3.1 Characterization of the kinetic behavior

In this work we analyze the kinetics of the three polypeptide systems, Ala6, chrg-Ala6, and cyc-Ala6, from their eigenvalue spectra and the eigenvectors of the transition matrix $\tilde{\boldsymbol{W}}$. This study proposes an alternative way to identify the macroscopic kinetic behavior by analyzing the transition matrix, rather than by following the propagation of a macroscopic property (*e.g.*, the average potential energy, $\langle E(t)\rangle$), analyzing its relaxation, and then fitting it to different decay functions. This new analysis will be compared with the results of a previous study, where several discrete timescales specifying each relaxation profile were detected by plotting $\mathrm{d}\log(\langle E(t)\rangle)/\mathrm{d}\log(t)$, $\langle E(t)\rangle$ being the average potential energy function.[16] Applying this analysis to a hierarchical dynamic process results in logarithmic oscillations where each represents, in the course of time, the contribution of yet another relaxation channel in the temporal decay patterns. The existence of several timescales was demonstrated by fitting the decays of the potential energy to a multiexponential function.

The time evolution of the probability vector (eqn. (4)), as well as of the average energy (eqn. (7)), displays multiexponential decays composed of n exponents where n is the number of conformations of each system. Of course, the number of important exponents characterizing the kinetics is reduced from n to a smaller number since some exponents have very small preexponential factors. Furthermore, some decay rates are so high that they are of little physical interest at present, *e.g.*, greater than 10^{13} s^{-1} (0.01 fs^{-1}). The timescale represented by exponent k is the inverse of the corresponding eigenvalue, *i.e.*, ${\lambda_k}^{-1}$. We present an analysis which enables us to find among the n possible timescales defined by the eigenvalues of the transition matrix the important ones that characterize the kinetics.

Each of the n relaxation modes contributes differently to the evolution of the probability of the minimum i and is given by the term $\sqrt{P_i^{\mathrm{eq}}}C^k S_i^k$ (eqn. (4)). These contributions can be positive or negative and depend on the initial and current population (eqn. (5)). A measure of the contribution of mode k, with eigenvalue λ_k, to the probability evolution of *all minima* (*i.e.*, to the total probability) is denoted by CP^k and takes into account all the contributions of the relaxation mode k to all n minima,

$$CP^k = \sum_i \left|\sqrt{P_i^{\mathrm{eq}}}C^k S_i^k\right| \tag{8}$$

Similarly, we define CE^k to be the contribution of mode k to the relaxation of the potential energy,

$$CE^k = \sum_i \left|\sqrt{P_i^{\mathrm{eq}}}E^k S_i^k\right| \tag{9}$$

The relative magnitudes of the CP^k and CE^k may indicate the important ('relevant') modes (eigenvalues) for the propagation of the probability and of the energy relaxation, respectively. In general, we do not expect a strong correlation between the modes responsible for the relaxations of the two different properties. If the relaxation profile is fitted by using a multiexponential function with different lifetimes τ_i, *i.e.*,

$$\langle E(t)\rangle - \langle E\rangle^{\mathrm{eq}} = \sum_i A_i \mathrm{e}^{-t/\tau_i}$$

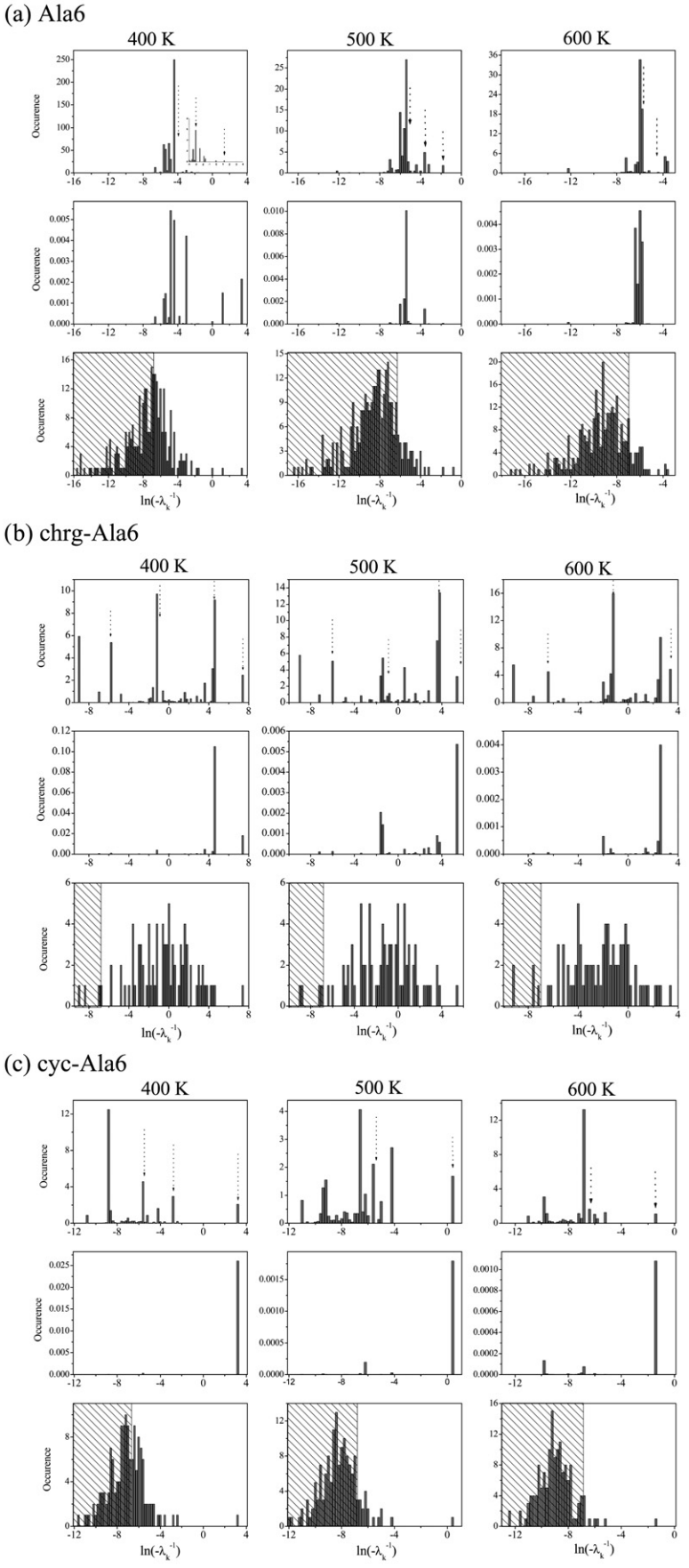

Fig. 1 Eigenvalue spectra at 400–600 K for three hexapeptides. The unweighted eigenvalue spectra are shown at the bottom panel and the spectra of the eigenvalues weighted by CE^k and CP^k factors are shown at the top and middle panels, respectively. The reciprocal eigenvalues $-\lambda_k{}^{-1} = \tau_k$ are presented in units of ns. The dashed arrows indicate the decay lifetimes, τ_j, obtained from the optimal multiexponential fit of the relaxation curves. The dashed regions contain unphysical eigenvalues that obey the relation $\lambda_k{}^{-1} < 10^{-3}$ ns. (a) Eigenvalue spectra for Ala6. (b) Eigenvalue spectra for chrg-Ala6. (c) Eigenvalues spectra for cyc-Ala6.

Table 1 The decay lifetimes, τ_j (in ns), obtained from the optimal multiexponential fit of the relaxation curves of each polypeptide at 400, 500, and 600 K. The number of exponents involved in each fit was determined by the behavior of the logarithmic oscillations

	Ala6			chrg-Ala6				Cyc-Ala6		
	τ_1	τ_2	τ_3	τ_1	τ_2	τ_3	τ_4	τ_1	τ_2	τ_3
400 K	0.024	0.12	2.83	0.0031	0.39	82	2110	0.0053	0.057	31.4
500 K	0.0071	0.026	0.18	0.0026	0.43	62	430	—	0.0051	1.51
600 K	0.0037	0.011	—	0.0017	0.31	26	—	—	0.0018	0.18

then the pre-exponential factors, A_i, are CE^k. Alternative calculations of CP^k and CE^k were performed by taking the absolute values of the sums of products in eqns. (8) and (9), instead of using the sum of the absolute values. Strong cancellations were manifested in the alternative scheme in the range of some relevant eigenvalues, which appear in the multiexponential time-dependent fit, and which lead to the disappearance (shrinking) of these contributions. Accordingly, we choose the presentation in terms of eqns. (8) and (9), which avoids extreme cancellations.

Fig. 1(a) describes the histograms of the eigenvalues where for the linear hexapeptide, Ala6, eigenvalue k is weighted by CE^k (top panel), and by CP^k (middle panel), and the entire eigenvalue spectra of the kinetic matrix with a weight of unity (bottom panel) are presented. The eigenvalues of the kinetic matrix (bottom panel) are all positive or zero. Figs. 1(b) and 1(c) are similar to Fig. 1(a) but for chrg-Ala6 and cyc-Ala6, respectively. The histograms of the entire eigenvalue spectra (the bottom panels of Figs. 1(a–c)) are very broad and include eigenvalues that represent both slow (few ms) and fast (few fs) events. The dynamics of all the systems includes processes described by large eigenvalues (small $\ln(\lambda_k{}^{-1})$ values) which correspond to fast processes, with no physical meaning for the dynamics of the systems at hand. In the present analysis we consider any eigenvalue as having physical meaning if its inverse is larger then 10^{-3} ns (1 ps). The lower temporal limit of $\tau_l = 1$ ps corresponds to a classical (harmonic) vibration frequency of $1/C\tau_1 = 30\ \mathrm{cm}^{-1}$, marking low-frequency intermolecular modes of the polypeptides. The 'irrelevant' region of the large eigenvalues, which obey the relation $\lambda_k{}^{-1} < 10^{-3}$ ns, is marked by diagonal lines. The spectra of the eigenvalues weighted by CE^k factors for Ala6 (top panel of Fig. 1(a)) are considerably narrower than the total eigenvalue spectra, and almost all the unphysical timescales have no importance for the dynamics. For chrg-Ala6 and cyc-Ala6 the spectra of the eigenvalues weighted by CE^k factors indicate that several fast modes have a contribution larger than zero.

The spectra for the three systems (Figs. 1(a)–(c)) are drastically filtered, indicating that not all the n eigenvalues have equal significance in the energy relaxation; rather, the decay can be described by a smaller set of eigenvalues. Arrows were added to the spectra to indicate the characteristic lifetimes as obtained by fitting the energy relaxations to multiexponential functions.[16] The number of arrows (characteristic times) were determined by the number of logarithmic oscillations found by the logarithmic derivative of the potential energy relaxation relative to time.[16] Tables 1 and 2 present the characteristic times of the multiexponential kinetics of each system at temperatures of 400, 500, and 600 K, as well as their preexponential factors. For cyc-Ala6 and chrg-Ala6, which are characterized by hierarchical dynamics, there is good agreement between the timescales found by fitting to a multiple exponential function and the eigenvalues with the largest contributions. Moreover, there is also a partial correlation between the relative heights of the contributions of the important eigenvalues and the preexponential factors found by the fitting. However, in some cases the CE^k factors of each eigenvalue fail to estimate the total contributions, since two similar sub-contributions with opposite signs may cancel each other out and thus decrease the total contribution. In addition, it is possible that the logarithmic oscillations fail to detect all the characteristic lifetimes involved in the decay and thus additional lifetimes, as suggested by the present analysis (for example the eigenvalue spectrum of chrg-Ala6 at 600 K), may result in improvement of the fitting properties.

With increasing the temperature there is an expected shift of the spectra of the eigenvalues to smaller values of $-\lambda_k{}^{-1}$, indicating shorter timescales. For Ala6 and cyc-Ala6 the shifts of the spectra, due to increasing the temperature, result in more unphysical time-scales and consequently fewer eigenvalues are involved in the dynamics. The observation that almost no temperature effect on the eigenvalue spectrum is detected for chrg-Ala6 suggests that the temperatures in this range (400–600 K) are not sufficient to enable escape from the trapping state. This behavior was previously observed for this system by projecting the probability distribution onto its energy landscape.[16] It was shown that at these temperatures the peptide is trapped in the native state. It should be mentioned that for Ala6 and cyc-Ala6 increasing the temperature results in populating different states beside the native one. The existence of a temperature effect on the kinetics can initially be reflected by the eigenvalue spectra.

The eigenvalue spectra of the three hexapeptides indicate that only for chrg-Ala6 and cyc-Ala6 (Figs. 1(b) and 1(c), respectively) the smallest eigenvalues at the three temperatures (the largest $\ln(-\lambda_k{}^{-1})$) are associated with the slowest decay channel (longest lifetime), while for Ala6 (Fig. 1(a)) the lifetime of the slowest decay channel is not described by the smallest eigenvalue. Recalling that the kinetics of chrg-Ala6 and cyc-Ala6 are more hierarchical than the kinetics of Ala6, it is suggested that for hierarchical kinetics the smallest eigenvalue characterizes the rate-determining step of the relaxation process. We conjecture that this observation is related to a structural constraint that exists in both

Table 2 The preexponential decay factors, A_j (in kcal mol^{-1}), obtained from the optimal multiexponential fit of the relaxation curves of each polypeptide at 400, 500, and 600 K

	Ala6			chrg-Ala6				cyc-Ala6		
	A_1	A_2	A_3	A_1	A_2	A_3	A_4	A_1	A_2	A_3
400 K	14.1	6.2	0.32	7.5	10.1	10.2	2.7	4.8	3.9	2.2
500 K	11.0	3.3	2.2	7.4	12.6	8.5	2.2	—	7.9	2.1
600 K	7.3	2.5	—	7.1	13.0	11.1	—	—	6.1	1.6

chrg-Ala6 and cyc-Ala6 (*i.e.*, electrostatic interaction and cyclization, respectively).

The spectra of the eigenvalues weighted by CP^k factors (middle panel in Figs. 1(a)–(c)) are similar to the spectra of the CE^k weighted eigenvalues. These spectra are much narrower and more filtered than the non-weighted spectra. Some of the eigenvalues found to be essential for the relaxation of the potential energy are also important in the evolution of the probability distribution.

3.2 The effect of the initial probability population

The effect of the initial population distribution on the dynamics obtained by solving the master equation is of interest and requires elucidation. One expects that populating different regions of the energy landscapes, as different initial conditions of the master equation, may result in different dynamics. We now address the question of the initial population by observing their effect on the (weighted) eigenvalue spectra. The evolving population distribution vector necessarily reflects the effect of the initial probability population on the dynamics, since the initial probability is introduced in the weights calculated by the C^k parameters, eqn. (5), and thus may make the evolution process sensitive to them. In order to examine the effect of the initial population on the characteristic dynamics and kinetics characteristic lifetimes we constructed the weighted eigenvalue spectra for different initial probability populations. Fig. 2 shows several CP^k weighted eigenvalue spectra for the three systems at 500 K. For Ala6, spectrum A was obtained for the initial population probability where only the highest energy state was populated and the spectrum F was obtained for equal populations of all the 280 states. Spectra B–E were obtained for equally populating the 10, 20, 50, 140 *highest* energy states of the Ala6 energy landscapes. It can be seen that the general properties of the spectra are very similar for all these initial populations with differences in the relative heights of the important eigenvalues. However, when the system has an initial population in the 50 *lowest* states (spectrum G), we see the spectrum quite differently: some additional small eigenvalues (slow processes) appear. The weighted eigenvalue spectrum can thus serve as a validation tool to examine the initial probability population. It should be mentioned that very similar characteristic times were obtained for the relaxation decays for Ala6 using initial probabilities A, B, and C.[16]

The effect of the initial probability distribution on the dynamics and on the master equation solution was also studied using the eigenvalue spectra for chrg-Ala6 and cyc-Ala6. For these two systems it appears again that if the higher states are populated then the spectra are very similar in a pattern analogous to the case of Ala6. However, when only low energy states are populated (the bottom of the energy landscape, spectra G and H of chrg-Ala6, and spectrum G of cyc-Ala6) then the spectra look very different. This is due to the exclusion of fast transitions from higher energy states to other lower states, since the top of the energy landscape is not populated and the dynamics, which in this case prevails, is among the low energy states and yields towards the global minimum.

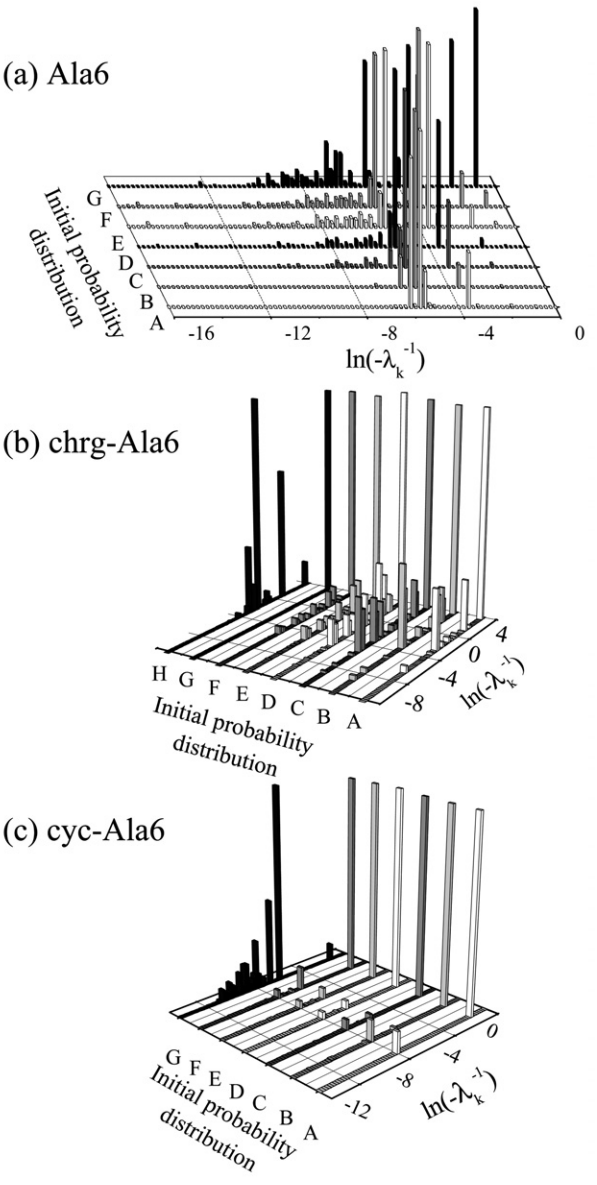

Fig. 2 Spectra of the CP^k weighted eigenvalues at 500 K for Ala6 (a), chrg-Ala6 (b), cyc-Ala6 (c). The seven spectra (A–G) for each of the three hexapeptides differ in the initial probability distributions. In all cases spectrum A was obtained for the initial population probability where only the highest energy state was populated, and spectrum F was obtained for equal populations of all the states that define the energy landscape (280, 86, and 148, for Ala6, chrg-Ala6, and cyc-Ala6, respectively). Spectra B–E were obtained for intermediate populations of the states, starting from the top of the energy landscape. For Ala6 spectra B–E were obtained for equally populating the 10, 20, 50, and 140 highest energy states. Spectra G and H were obtained by initially populating the 20 and 10 states with the lowest energies.

3.3 Relaxation pathways and the energy landscape

An important question regarding the dynamics on a complex energy landscape is whether the temporal relaxation patterns represent sequential or parallel processes. In the case of sequential processes, each decay channel corresponds to a different region of the energy landscape. Here, the topography and topology of the energy landscape dictate the hierarchy of the relaxation channels. A cursory examination of sequential dynamics may suggest that fast processes originate from transitions at the upper part of the energy landscape and that slow processes are associated with transitions at the bottom regions of the energy landscape towards the global minimum. On the other hand, in the case of parallel processes, we may expect only a weak dependence on the energy with different decay channels and it is likely that several pathways will be simultaneously populated with different probabilities.

To address this question the contribution of each relaxation mode (eigenvalue) to the time evolution of the energy relaxation of each minimum on the energy landscape was tested. This approach enables correlating the eigenvalues with the minima constituting the energy landscape. The contribution of the kth eigenvalue, λ_k, to the energy evolution of the minimum (state) i is given by

$$\Gamma_i^k = \sqrt{P_i^{eq}} E_i C^k S_i^k \qquad (10)$$

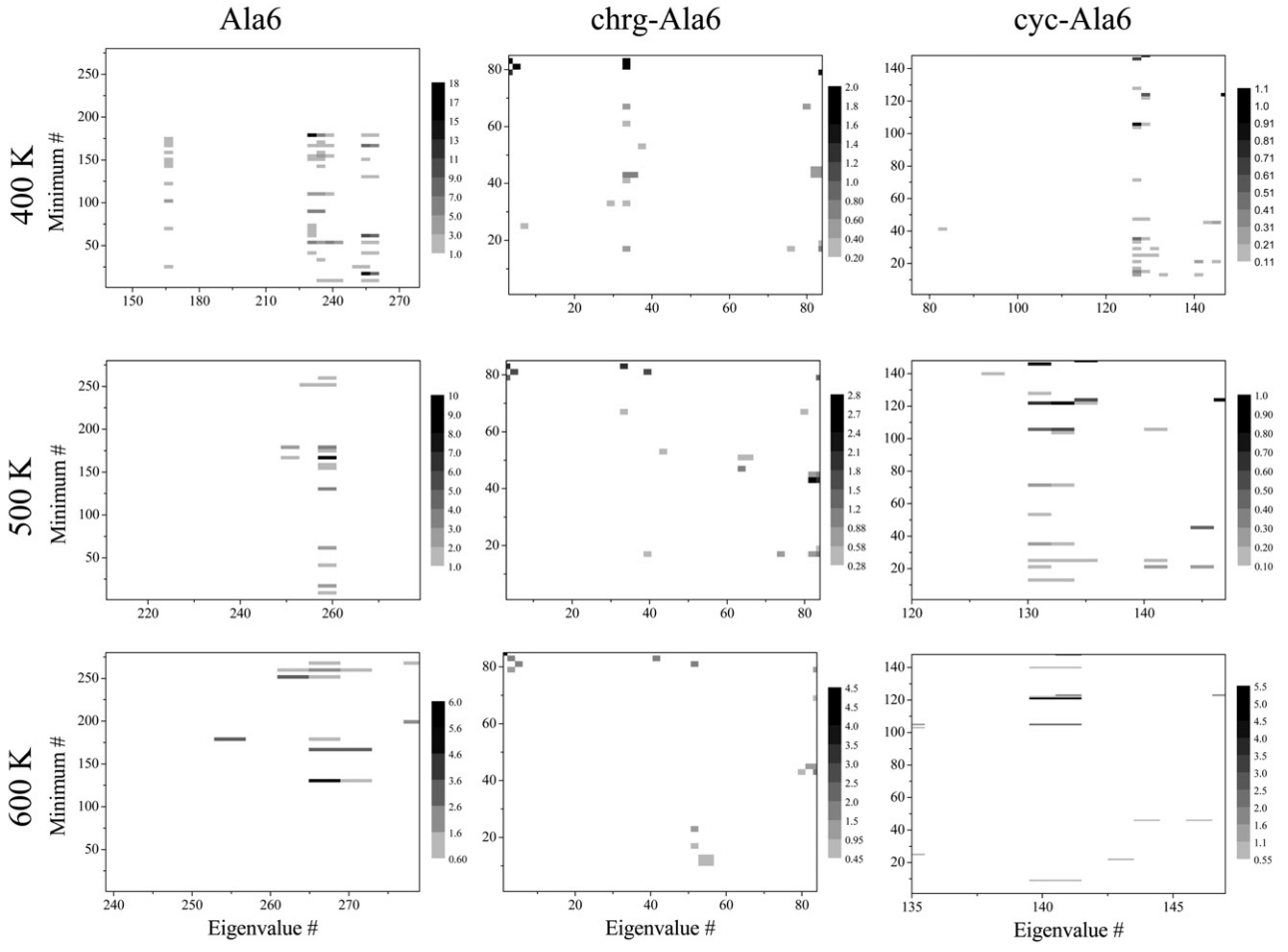

Fig. 3 The Γ_i^k contribution [the contribution of the kth eigenvalue, λ_k (in units of ns^{-1}), to the energy evolution of the minimum i, eqn. (10)] for the three hexapeptides at 400–600 K. Only the eigenvalues with physical timescales (>1 ps) are presented. Accordingly, for Ala6 142 ($T = 400$ K), 69 ($T = 500$ K), and 41 ($T = 600$) eigenvalues out of its 280 eigenvalues are presented, for chrg-Ala6 82 ($T = 400$ K), 82 ($T = 500$ K), and 80 ($T = 600$ K) eigenvalues out of the 85 eigenvalues are included and for cyc-Ala6 66 ($T = 400$ K), 28 ($T = 500$ K), and 13 ($T = 600$ K) eigenvalues out of its 148 eigenvalues are shown. The eigenvalues are ordered according to their values starting with the smallest λ_k (fastest process). The minima are ordered by their potential energy, starting with the global minimum as index 1.

Thus the components of each CE^k (eqn. (9)) are analyzed and determine which minima are involved in the relaxation channel characterized by the kth eigenvalue. Fig. 3 shows the contributions Γ_i^k for the three molecular systems in the temperature range 400–600 K, where magnitudes of the contributions are represented by gray scaled colors. In these figures only the eigenvalues with physical timescales (>1 ps) are presented. Accordingly, for Ala6 142 ($T = 400$ K), 69 ($T = 500$ K), and 41 ($T = 600$) eigenvalues out of its 280 eigenvalues are presented, for chrg-Ala6 82 ($T = 400$ K), 82 ($T = 500$ K), and 80 ($T = 600$ K) eigenvalues out of the 85 eigenvalues are included and for cyc-Ala6 66 ($T = 400$ K), 28 ($T = 500$ K), and 13 ($T = 600$ K) eigenvalues out of its 148 eigenvalues are shown. Irrespective of the molecular system, it is shown that among the eigenvalues on the physical relevant timescale, there are only a few eigenvalues which contribute to the energy relaxation dynamics of any minimum. This pattern again demonstrates the filtering effect of the eigenvalues, as discussed before.

The relaxation dynamics which involves the filtering effect of the eigenvalues can result in narrow 'islands' of minima (states) with similar energies, or, alternatively, a broad distribution of minima (states) corresponding to a few eigenvalues. Fig. 3 clearly demonstrates that the sparsely spread eigenvalues participating in the relaxation kinetics contribute to a broad spread of minima with different potential energies. Accordingly, each significant eigenvalue (or, alternatively, a group of eigenvalues with similar lifetimes) is uncorrelated with a small region on the energy landscape but describes a channel that may span the entire range of the potential energy on the energy landscape. Though similar minima can be involved in two parallel pathways with different timescales the population probability of each minimum in these two pathways is different. Especially for chrg-Ala6, it is worth noting that, while many minima with a broad range of potential energies participate in the relaxation channel, there are some minima that are excluded from these pathways. This is due to the topological and multidimensional features of the polypeptide energy landscapes. Two minima with similar energies can have different connectivities and consequently may be involved in different relaxation channels.

In the context of parallel relaxation dynamics, we note that the energy relaxation of the three hexapeptides onto their underlying multidimensional energy landscapes is characterized by multiple pathways, where each relaxation channel has a specific characteristic lifetime and spans a large range of minima. The existence of parallel pathways in the folding of "small" systems, such as peptides, reflects the multidimensionality of their underlying energy landscapes and that protein folding should not be described by a single pathway onto a two dimensional surface. The pathways do not only differ in the dimensions in which they take place and in their timescales, but also in the probability populations of each of the minima that construct them, and consequently each pathway is characterized by a different weight, as reflected by its pre-exponential factor.

To conclude, an alternative way was presented to interpret the solutions of the master equation and to extract detailed information about the dynamics of complex systems. This method was used here to filter the important relaxation modes out of hundreds of nonphysical modes and to characterize the multiexponential kinetics previously found for the studied hexapeptide systems. The relaxation modes (*i.e.*, characteristic timescales) and their contributions (*i.e.*, preexponential factors) to the kinetics, as found by this method, are in good agreement with those found by following the propagation of the energy relaxation and fitting them to decay functions. This method provides a relatively simple way to explore the dynamics of complex systems from the eigenvalues and eigenvectors obtained from the solution of the master equation, without the need of considering the time evolution of observables. One may expect that different filtering effects will be manifested for eigenvalues corresponding to multiexponential, stretched exponential, and power-law kinetics. The method was found to be useful to correlate each relaxation pathway with the minima constituting the energy landscape and to explore the effects of temperature and the initial population distribution on the dynamics.

References

1 A. Fersht, *Structure and Mechanism in Protein Science: A Guide to Enzyme Catalysis and Protein Folding*, Freeman, New York, 1999.
2 M. Gruebele, *Annu. Rev. Phys. Chem.*, 1999, **50**, 485–516.
3 T. Metzler, J. Klafter, J. Jortner and M. Volk, *Chem. Phys. Lett.*, 1998, **293**, 477–484.
4 A. Plonka, *Chem. Phys. Lett.*, 2000, **328**, 124–128.
5 H. K. Nakamura, T. N. Sasaki and M. Sasai, *Chem. Phys. Lett.*, 2001, **347**, 247–254.
6 H. Frauenfelder and P. G. Wolynes, *Science*, 1985, **229**, 337–345.
7 H. Frauenfelder and P. G. Wolynes, *Phys. Today*, 1994, **47**, 58–64.
8 R. S. Berry and R. E. Kunz, *Phys. Rev. Lett.*, 1995, **14**, 3951.
9 R. E. Kunz and R. S. Berry, *J. Chem. Phys.*, 1995, **103**, 1904.
10 K. D. Ball, R. S. Berry, R. E. Kunz, F.-Y. Li, A. Proykova and D. J. Wales, *Science*, 1996, **271**, 963.
11 D. J. Wales, M. A. Miller and T. R. Walsh, *Nature*, 1998, **394**, 758–835.
12 M. A. Miller and D. J. Wales, *J. Chem. Phys.*, 1999, **111**, 6610.
13 D. J. Wales, J. P. K. Doye, M. A. Miller, P. N. Mortenson and T. R. Walsh, *Adv. Chem. Phys.*, 2000, **115**, 1–111.
14 O. M. Becker and M. Karplus, *J. Chem. Phys.*, 1997, **106**, 1495–1517.
15 Y. Levy and O. M. Becker, *J. Chem. Phys.*, 2001, **114**, 993–1009.
16 Y. Levy, J. Jortner and O. Becker, *J. Chem. Phys.*, 2001, **115**, 10 533–10 547.
17 Y. Levy, J. Jortner and O. M. Becker, *Proc. Natl. Acad. Sci. USA.*, 2001, **98**, 2188–2193.
18 F. Despa and R. S. Berry, *Eur. Phys. J. D*, 2001, **16**, 55.
19 F. Despa and R. S. Berry, *J. Chem. Phys.*, 2001, **115**, 8274.
20 J. D. Bryngelson, J. N. Onuchic, N. D. Socci and P. G. Wolynes, *Proteins: Struct. Funct. Genet.*, 1995, **21**, 167–195.
21 J. N. Onuchic, Z. Luthey-Schulten and P. G. Wolynes, *Annu. Rev. Phys. Chem.*, 1997, **48**, 539–594.
22 H. S. Chan and K. A. Dill, *Proteins: Struct. Funct. Genet.*, 1998, **30**, 2–33.
23 C. M. Dobson, A. Sali and M. Karplus, *Angew. Chem.*, 1998, **37**, 868–893.
24 K. A. Dill, *Protein Sci.*, 1999, **8**, 1166–1180.
25 H. Frauenfelder and B. McMahon, *Ann. Phys. (Leipzig)*, 2000, **9**, 655–667.
26 K. D. Ball and R. S. Berry, *J. Chem. Phys.*, 1998, **109**, 8557–8572.
27 M. A. Miller, J. P. K. Doye and D. J. Wales, *Phys. Rev. E.*, 1999, **60**, 3701–3718.
28 R. Czerminski and R. Elber, *J. Chem. Phys.*, 1990, **92**, 5580–5601.
29 P. N. Mortenson and D. J. Wales, *J. Chem. Phys.*, 2001, **114**, 6443–6454.
30 N. G. v. Kampen, *Stochastic Processes in Physics and Chemistry*, North Holland, Amsterdam, 1981.
31 I. Oppenheim, K. E. Shuler and G. H. Weiss, *Stochastic Processes in Chemical Physics: The Master Equation*, The MIT Press, Cambridge, Massachusetts, and London, UK, 1977.